

## Particle chains in a dilute dusty plasma with subsonic ion flow

O. Arp,<sup>1</sup> J. Goree,<sup>2</sup> and A. Piel<sup>1</sup><sup>1</sup>*Institut für Experimentelle und Angewandte Physik, Christian-Albrechts-Universität zu Kiel, D-24098 Kiel, Germany*<sup>2</sup>*Department of Physics and Astronomy, The University of Iowa, Iowa City, Iowa 52242, USA*

(Received 7 December 2011; revised manuscript received 2 March 2012; published 17 April 2012)

Chains of charged dust particles are observed aligned with a subsonic ion flow. These chains are found in dilute regions, near the midplane of a parallel-plate radio-frequency plasma under microgravity conditions. The argon ion flow speed near these chains was estimated to be of order  $10^2$  m/s, corresponding to an ion acoustic Mach number  $M < 0.1$ . The chains were observed to be stable in both the longitudinal and transverse directions. This stability suggests that there is a transverse restoring force. The transverse components of the ion-drag force or electrostatic wake-field forces could provide such a stabilizing effect. The chain appears to terminate with a final dust particle that is located in a dilute region; this observation suggests a possible attractive force in the longitudinal direction in the presence of a subsonic ion flow.

DOI: [10.1103/PhysRevE.85.046409](https://doi.org/10.1103/PhysRevE.85.046409)

PACS number(s): 52.27.Lw

### I. INTRODUCTION

A dusty (complex) plasma is a mixture of charged micron-sized particles of solid matter, electrons, ions, and neutral gas. In laboratory plasmas, micron-sized solid “dust” particles gain a negative electrical charge of thousands of elementary charges [1]. Experiments with dusty plasmas are often performed using a low-pressure radio-frequency (rf) gas discharge in parallel-plate geometry. The space between the electrodes is divided into a main plasma, where most electrons and ions are generated, and sheaths, which are boundaries near the electrodes. Electric fields are stronger by at least an order of magnitude in the sheaths as compared to the main plasma. The ions and dust particles are more massive, so that they do not respond to the rf fields, but only to time-averaged (ambipolar) dc electric fields that are also present.

Ions are generated by ionization of the argon gas [2]. The density gradient and the dc electric field  $E_{dc}$  causes ions to flow away from the main plasma and toward the electrodes on the chamber’s boundaries. The ion thermal speed  $v_{T,i} = (k_B T_i / m_i)^{1/2}$  is much slower than the ion acoustic speed  $c_s = (k_B T_e / m_i)^{1/2}$ , where  $m_i$  is the ion mass, because the electron temperature  $T_e$  is about two orders of magnitude higher than the ion temperature  $T_i$ . The flow is said to be subsonic when the ion-acoustic Mach number  $M \equiv v_i / c_s < 1$ , as is typical in the main plasma but not in the sheath.

A dust particle disturbs its surrounding electrons and ions in a screening region with a typical size [3,4] on the order of 0.1 mm. Due to the ion flow, this screening region is not spherical, but has an excess of positive charge downstream of the dust particle. This ion wake field can modify the interaction between two particles so that it is anisotropic [1].

This anisotropic particle interaction in the presence of streaming ions may cause an alignment of dust particles along the ion flow direction. *Theoretical* studies of chains in an ion flow include a simulation by Lampe *et al.* [5], who used a dressed particle code that assumes small-angle ion deflections as an input to a molecular-dynamics simulations. They found that a few particles can form a stable chain of several particles, when they are isolated from other particles.

Chainlike configurations of dust particles have been seen previously in many dusty plasma *laboratory experiments* that

showed, e.g., vertical particle chains in the sheath region of capacitively coupled rf plasmas [6–9] and in the periphery of an inductively coupled rf plasma [10]. In these experiments Earth’s gravity causes micrometer-sized dust particles to sediment into regions of the discharge where a large  $E_{dc}$  levitates them and where ions flow at supersonic speeds.

Under microgravity conditions the particles tend to fill the main plasma, where  $E_{dc}$  and  $v_i$  are much smaller than, e.g., in an electrode sheath. Microgravity experiments with dusty plasmas have been performed on sounding rockets [11], in low Earth orbit [12,13], and on parabolic aircraft flights [14,15]. In these experiments, aligned particles have been reported mainly for nonsteady conditions, e.g., when driving the ion flow in alternating directions by means of external electric fields [16], and in counterpropagating particle flows [17,18].

In this paper, we will present observations of chainlike configurations of particles in dilute regions of a dusty plasma under microgravity conditions. The particle chains appear spontaneously and are observed midway between the two parallel-plate electrodes, where the particles are immersed in an extremely slow subsonic ion flow.

### II. EXPERIMENT

The experiments were performed in parabolic aircraft flights. The IMPF-K [14] and IMPF-K2 [19] devices were used in the 2007 and 2009 flight campaigns, respectively. Both devices have parallel-plate circular stainless-steel electrodes of 80 mm diameter, separated by a gap of 30 mm (Fig. 1). The electrodes were powered in a push-pull mode at 13.56 MHz with peak-to-peak rf voltages of 45 to 70 V, without any dc bias between the electrodes. Argon at a pressure of 15, 30, or 50 Pa was used, without gas flow. The two chambers differ only in their electrode configuration: the IMPF-K electrodes are each segmented into a central disk of 30 mm diameter surrounded by two electrically connected concentric rings. The rf voltage on the disk and the rings can be adjusted independently. The IMPF-K2 electrodes are not segmented, i.e., the same voltage was applied everywhere on the electrode’s surface.

After forming the plasma, melamine-formaldehyde polymer particles were introduced by electromagnetically agitated dust dispensers. The particle diameter was either 6.8 or

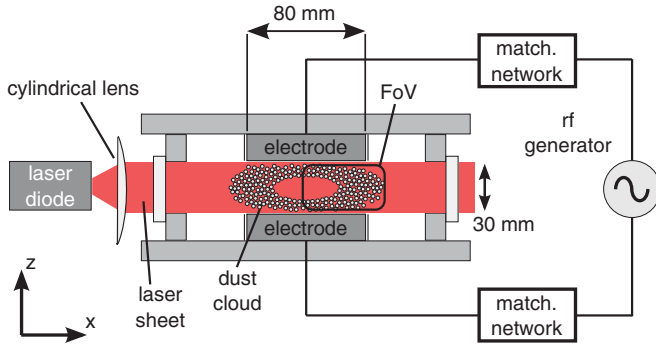


FIG. 1. (Color online) Cross-sectional sketch, IMPF-K2 device. The dust is illuminated by a vertical laser sheet. The camera's field of view is marked by the solid rectangle (FoV).

$9.55 \mu\text{m}$ . During microgravity conditions, dust particles settled in a nearly steady state, without vortices or other flows. A cross section of the 3D dust cloud was illuminated by a  $500\text{-}\mu\text{m}$ -thick sheet of laser light from a  $50\text{-mW}$  red diode laser of wavelength  $660 \text{ nm}$ . Particles within this illuminated region were imaged by a camera viewing at  $90^\circ$  to the laser sheet. The camera's field of view was  $61.1 \times 38.9 \text{ mm}$  and  $57.9 \times 36.8 \text{ mm}$  in the 2007 and 2009 campaigns, respectively. Earlier investigations [14,19] in the same setup showed that dust-density waves are self-excited below a critical gas pressure of  $\approx 35 \text{ Pa}$  due to streaming ions.

To estimate the plasma parameters, we simulated the plasma using a fluid model. In the region where we observe chains in the experiment (within  $0.4 \text{ cm}$  of either side of the midplane and at radii between  $1.5$  and  $3.5 \text{ cm}$ ) we find an ion flow speed of  $\approx 10^2 \text{ m/s}$ . This very slow ion flow speed is comparable to the ion thermal speed  $v_{T,i} \approx 250 \text{ m/s}$ , assuming  $T_i \approx 300 \text{ K}$ . The Mach number in this same region is in the range  $0.02 < M < 0.1$ . Details of the simulation, and a discussion of how these results for the ion speed are accurate only to within about a factor of 2, are presented in the Appendix.

To detect the direction of ion flow, we will rely on two signatures that are visible in the dust clouds: dust-density waves and voids. For  $M < 0.3$  the wave propagation is expected to align with the ion flow [20]. Thus, when wave fronts are visible, they indicate the ion flow direction. Voids are particle-free regions sometimes found near the center of the plasma, especially when the plasma is powered by large-amplitude radio-frequency fields [21–26]. These voids are sustained under steady conditions by a balance of inward electric forces and outward ion-drag forces and have a distinctive boundary, which is generally perpendicular to the ion flow [27].

In this paper, we will use both the orientation of the void boundary and the orientation of wave fronts (when they are present) to indicate the direction of ion flow.

### III. RESULTS

We present images of anisotropic chains of dust particles, aligned in the radial direction. These chains are located in a dilute region, i.e., in a space where the nearest-neighbor distance is smaller along a chain than perpendicular to it. When

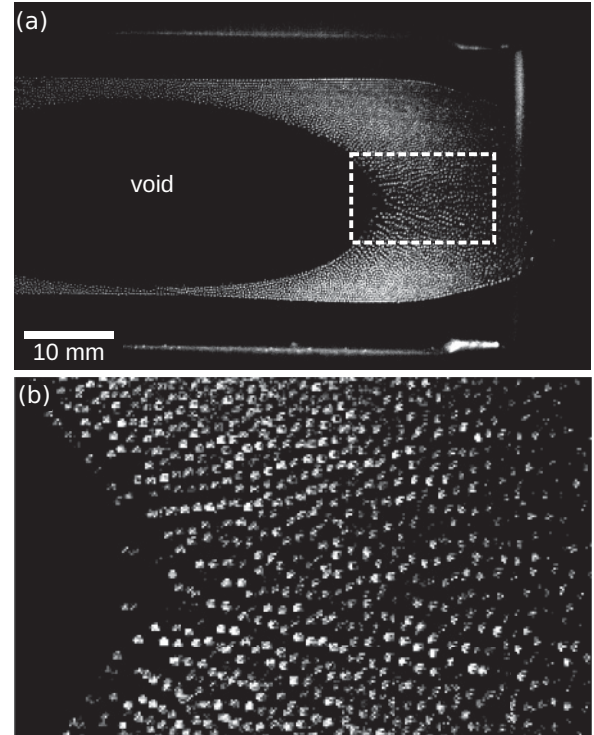


FIG. 2. (a) Chains, with a higher gas pressure. This image is a vertical cross section through the dust cloud. The dust-free “void” region marks the center of the discharge. Particles in the dilute region (dashed rectangle) centered around the midplane of the discharge are aligned in chains. (b) Magnification of the dashed region of interest. Parameters were as follows: particle diameter  $9.55 \mu\text{m}$ , argon pressure  $50 \text{ Pa}$ , rf amplitude  $50V_{pp}$  (IMPF-K2 chamber).

it occurs, this dilute region is found near the midplane halfway between the two electrodes. The chains are found both in the presence and in the absence of waves. However, chains are not ubiquitous, as we will demonstrate with an example that exhibits no dilute region and no chains.

As our first example, in Fig. 2(a) we see chains that appear in a dilute region near the midplane in a dust cloud. This image, which was recorded in the 2009 campaign, shows about half of a full cross section of the dust cloud. The void on the left side of the image marks the center of the discharge. White spots in this image are dust particles, which can be resolved individually. A magnification of the dashed region of interest is shown in Fig. 2(b). The particle spacing measured from the image helps in quantifying the anisotropy of the arrangement of particles. In the dilute region, the average particle spacing within a chain is  $342 \pm 4 \mu\text{m}$  parallel to the chain, but  $492 \pm 3 \mu\text{m}$  perpendicular to it. In the dense regions of the dust cloud, above or below the dilute region, the particle spacing is  $277 \pm 4 \mu\text{m}$ . Thus, in the dilute region on the midplane, one chain is separated from another by a considerably larger distance than the spacing of particles within a chain. The chains in Fig. 2 consist of 10 or more dust particles. They are mostly straight, with some slight bending and occasional bifurcations. In the video corresponding to Fig. 2, we observed that the chains are stationary, with little overall drift due to small accelerations of the aircraft. Based on the shape of the void and the dc

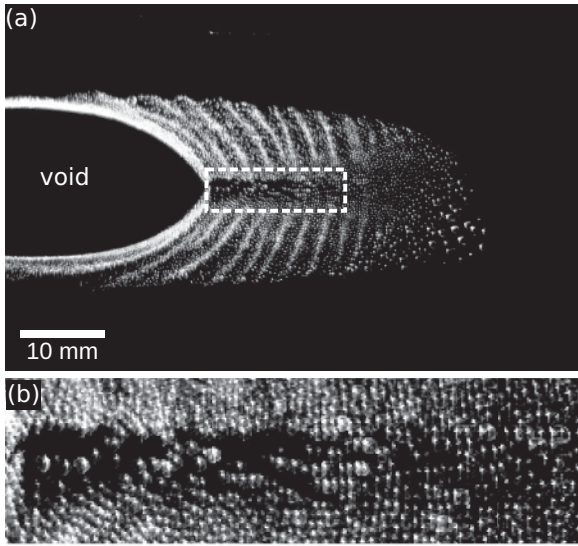


FIG. 3. (a) Chains, with a lower gas pressure. Self-excited dust-density waves are also present, and propagate from the “void” region outward. Particle chains are observed in a dilute gap (dashed rectangle) centered around the midplane of the discharge. (b) Magnification of the dashed region of interest. Parameters were as follows: particle diameter  $6.8 \mu\text{m}$ , argon pressure 15 Pa, rf amplitude  $70V_{pp}$  in the center and  $50V_{pp}$  in an outer ring (IMPF-K chamber).

symmetry of the electrode, we expect that the ion flow is directed radially outward in the dilute region, which is the same direction in which the chains are aligned.

As our second example, in Fig. 3(a) we see chains that are again located in a dilute region on the midplane. In this example, self-excited dust-density waves are present because the argon gas pressure of 15 Pa was sufficiently low. The wave fronts are seen as curved bands of compression and rarefaction in the dust cloud, with a wavelength of about 2 mm. Because wave fronts are a signature of the direction of ion flow, we can conclude from Fig. 3(a) that in the midplane the direction of the ion flow is again radially outward. This direction is as expected from the topology of the dc electric field  $E_{dc}$  that drove the ion flow and which should have a mirror symmetry with respect to the midplane.

Inspecting the video corresponding to Fig. 3, we determined that the length of the chains is generally 10 or fewer particles. The particle spacing in the dilute region is again smaller in the direction parallel to the chain as compared to the particle spacing perpendicular to the chains. In the dashed region of interest that is magnified in Fig. 3(b), the average particle spacing is  $312 \pm 7 \mu\text{m}$  parallel to the chain, while in the perpendicular direction the spacing is about twice as large. We can compare these values to the smaller particle spacing of  $269 \pm 5 \mu\text{m}$  a few mm above or below the dilute region in Fig. 3(b). Different from Fig. 2, in Fig. 3 the chains are not stationary in the dilute region but slowly drifting. By viewing the video, we found that small accelerations of the aircraft caused particle chains to detach from the denser clouds above or below the dilute gap. After a newly formed chain is detached into the dilute gap, it drifts slowly in the radially outward direction, at typically 3.6 mm/s, and vertically at about 1.6 mm/s.

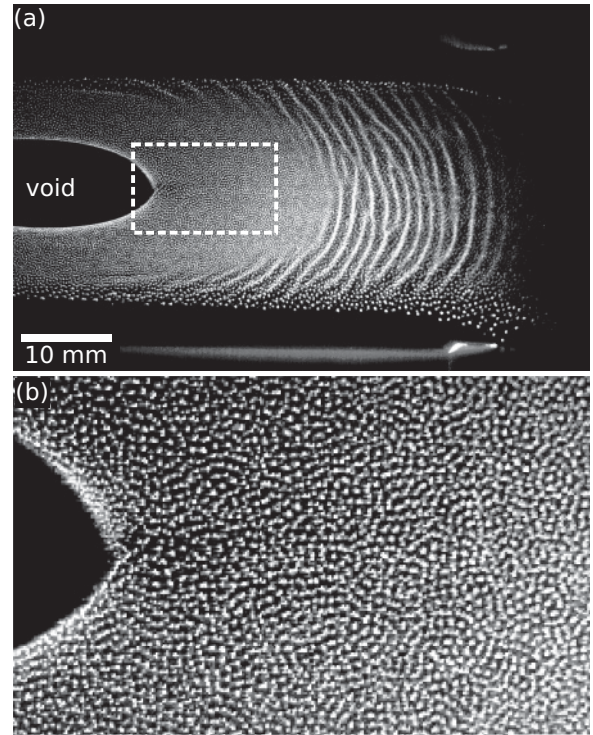


FIG. 4. (a) Dust cloud without chains or dilute region. (b) Magnification of the dashed region of interest. The average particle spacing on the midplane, between the void and the wave, is  $259 \pm 3 \mu\text{m}$ . Parameters were as follows: particle diameter  $9.55 \mu\text{m}$ , argon pressure 30 Pa, and rf amplitude  $45V_{pp}$  (IMPF-K2 chamber).

Two noteworthy observations regarding Fig. 3 are that the chains are isolated from each other, and that they seem to begin and end in the gap. Because we only observe a thin slice of the three-dimensional dust cloud, we are unable to exclude the possibility that these chains are connected to larger bodies of particles outside the gap rather than terminating within the gap, but such a possibility seems unlikely when inspecting the motion of the chains. If the chains do indeed terminate within the gap, the stability of the last particle in the chain suggests an attractive force, because otherwise a purely repulsive interparticle force would cause the last particle in the chain to be expelled from the chain into the surrounding dilute region. We discuss this possibility of an attractive force in Sec. IV.

In Fig. 4 we present an example demonstrating that chains are not ubiquitous. The magnification in Fig. 4(b) reveals no conspicuous chains. There is also no indication of a dilute region on the midplane. One of our main results is that chains appear in dilute regions, as seen in Figs. 2 and 3, but are absent when there is no dilute region, as shown in Fig. 4. This observation suggests that the conditions present in a dilute region are favorable for chain formation. However, we do not know what these conditions are, since we have no *in situ* measurements in this dilute region. Phenomenologically, we note that the dilute region’s appearance depends on the gas pressure, i.e., the mean-free path for collisions with neutral gas atoms. Dust-free simulations, like the one we present in the Appendix (Fig. 5), generally do not reveal anything

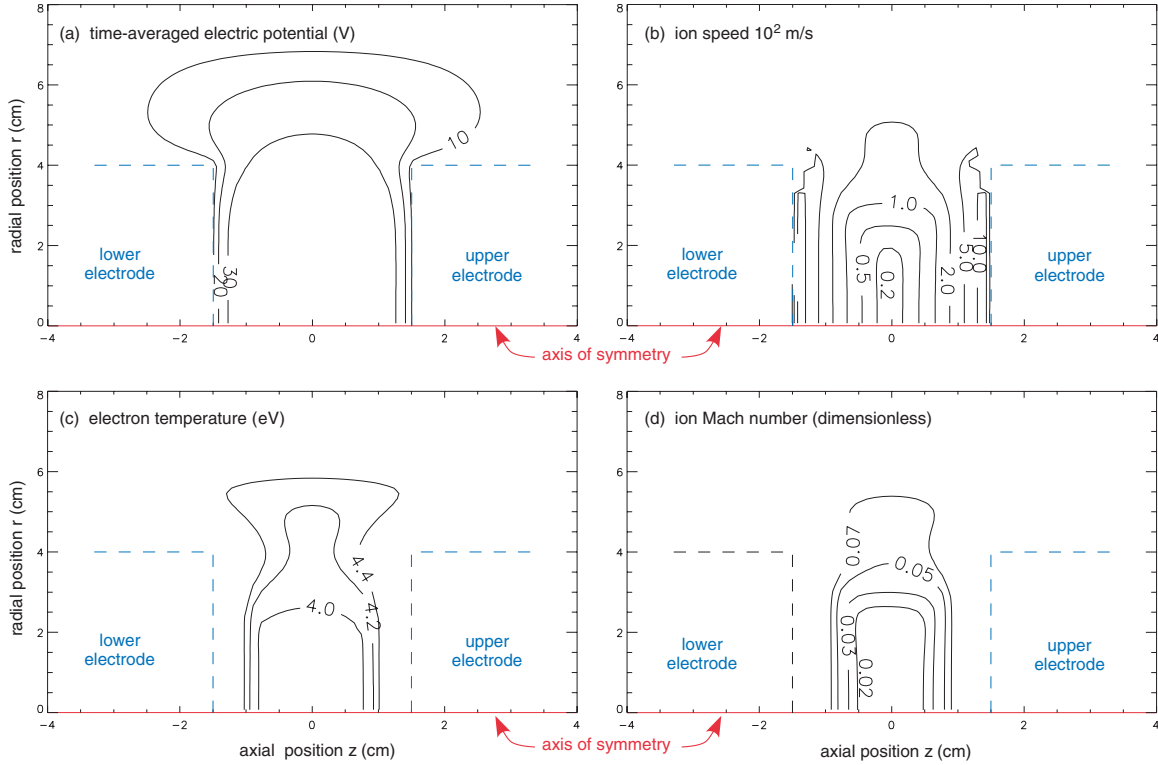


FIG. 5. (Color online) Fluid simulations of plasma parameters, neglecting the effect of dust. The chamber is cylindrical, with concentric electrodes; its axis of symmetry is the bottom of each graph at  $r = 0$ , and the midplane is at  $z = 0$ . The region of interest is approximately  $1.5 < r < 3.5$  cm and  $|z| < 0.4$  cm. Here, the dc electric potential (a) has only small gradients, which are purely radial. The corresponding small radial dc electric field drives a slow ion flow speed  $v_i$  (b) of order  $10^2$  m/s. Using electron temperature results from the simulation (c), in (d) we calculate the Mach number  $M = v_i/c_s$  and find that the flow is highly subsonic in the region of interest.

unusual on the midplane that might account for the dilute region. Simulations that include dust show, to the best of our knowledge, only a hint of a dilute region, as in Fig. 4 of Land and Goedheer [26].

#### IV. DISCUSSION

We have observed the formation of dust particle chains in low-speed ion flows in a dusty plasma. Our simulation in the Appendix indicates that  $v_i$  is subsonic, with a Mach number  $M < 0.1$  in the regions where we observed chains. The experimental design yielded an ion flow as slow as we can practically make it in a parallel-plate rf plasma. This was accomplished by two features of the experiment that contribute to achieving a small dc electric field, and therefore a small ion flow velocity. First, we used microgravity conditions to suspend the dust cloud in the central region of a plasma, where dc electric fields are weaker than in an electrode sheath. Second, we made observations near the midplane of the plasma using a chamber that had dc electrical symmetry for its top and bottom halves. This symmetry requires that the vertical dc electric field component should vanish, so that only radial dc electric fields would remain. We also presented a counterexample showing that a subsonic flow speed is a necessary but not sufficient condition for chain formation. In Fig. 4, chains were absent in the same midplane region where we observed them in Figs. 2 and 3. A condition that favors isolated chains is a dilute region on the midplane.

The key experimental observations we will discuss below are as follows: (1) chains parallel to a subsonic ion flow, (2) transverse stability of the chain, and (3) longitudinal stability of the chain. Our first observation, the formation of chains, indicates the presence of an interparticle force that is anisotropic. Since the chains are aligned with the ion flow, it is natural to attribute the anisotropy to that ion flow, which in this experiment was close to the ion thermal speed and much less than the ion acoustic speed. The remaining two observations center on the idea of stability. There must be restoring forces that provide stability so that a chain does not spontaneously disassemble when it is disturbed in the transverse or longitudinal directions. For the longitudinal direction, the restoring force must be attractive if the chain terminates in a dilute region.

To account for the transverse stability, we consider forces between two dust particles that are mediated by an ion flow. Here, the upstream particle acts as an electrostatic lens that focuses the ion flow, yielding a net positive space charge in the wake of the upstream particle. There are different ways of calculating the force on the downstream particle: When the force is derived from following the ion trajectories and by summing up the momentum transfer, the effect on the downstream particle is named ion-drag force. When a snapshot of all the simultaneous positions of ions in the self-consistent flow around the two-particle system is used, the force is called the wake-field attraction. We review briefly three theoretical and simulation papers that consider the transverse component

of these two forces. Lapenta [28] initiated this line of research by considering a two-particle system where the downstream particle is radially displaced from the axis of the flow. He recognized that there could be a stabilizing transverse force acting on the downstream particle and estimated the value of this force from the longitudinal part of the ion-drag force, for  $M = 1.5$ . Piel [29] extended Lapenta's ion-drag calculations and pointed out that the transverse part of the ion-drag force becomes significant as soon as the flow is no longer symmetric about the axis of this two-particle system, when the lower particle is displaced. Piel performed calculations for various ion flow speeds, including subsonic flows, to predict the magnitude of the transverse restoring force. Hutchinson [30] performed a particle-in-cell (PIC) simulation for  $M = 1$ , which resulted in a net transverse restoring force from the anisotropic structure of the wake field. These three authors took different approaches in their calculation methods and in the parameters they chose. While there is agreement that a stabilizing transverse force can occur, further simulations will be necessary to transfer the results from isolated two-particle systems to the present situation of chain formation in a dilute many-particle dust system.

Considering now the longitudinal stability, we note that our observation of chains indicates that interparticle forces are anisotropic. We now ask whether the evidence indicates that this anisotropic force is purely repulsive in the longitudinal direction, or whether it reverses direction and becomes positive at some distance. The primary observation of interest here is in Fig. 3, where it appears that the chains terminate with a last particle in a dilute region. In this case, the longitudinal force must actually be attractive, at the interparticle distances of about  $300 \mu\text{m}$  observed in Fig. 3. Although most of the theoretical literature for ion wake fields is for *supersonic* flows, there are indications that ion wake fields also occur for *subsonic* flows and that they can be attractive. We mention here three calculations of wakes in subsonic flows. First, Lampe *et al.* [31] reported that while the ion wake is mostly concentrated in a Mach cone behind the dust particle for supersonic flows, wake structures also occur for subsonic flows. The longitudinal gradient of the electric potential reverses direction in a subsonic wake field in Fig. 5 of Lampe *et al.* [31] for  $M = 0.5$ . Second, Guio *et al.* [32] reported collisionless PIC simulations at  $M = 0.42$  and  $0.75$ , and they remarked upon a noticeable variation of the electric potential in the wake that makes a long-range attraction possible, provided the electron-ion temperature ratio  $T_e/T_i$  is large. Third, recent PIC simulations of Hutchinson [33] at  $M = 0.5$  and  $0.8$  showed attractive wake potentials and revealed the importance of nonlinear effects for the structure of the wake.

More work, both experimental and theoretical, is needed to answer several questions raised here. Experiments with three-dimensional imaging would be helpful to eliminate any remaining uncertainties of the shape of the chains. Theoretical or simulation work in the subsonic-flow regime would also be helpful to identify the reasons for the transverse and longitudinal stability of the chains we observed. There is especially a need for more simulations for  $M < 0.1$  as in our experiment to identify the dominant transverse restoring force, and to quantify it.

## ACKNOWLEDGMENTS

Work performed in Iowa was supported by NASA and NSF. Work in Kiel was supported by DLR under Grant No. 50WM0739/50WM1039, by ESA, and partially by DFG TR-24/A2.

## APPENDIX: SIMULATION OF ION-FLOW CONDITIONS

To estimate the ion-flow speed, we performed a simulation using the SIGLO-2D code [34,35]. The plasma is modeled as coexisting fluids of electrons, ions, and a background of neutral gas. We used the dimensions of the experimental chamber, with 50-Pa argon and a 13.56-MHz sinusoidal wave form with a peak-to-peak voltage of 50 V. The simulation assumes cylindrical symmetry for the chamber, as in the experiment.

Simulation results are shown in Fig. 5. In the considered pressure regime the ion flow is governed by frequent collisions between ions and neutral gas atoms. From the time-averaged dc electric field [Fig. 5(a)] we calculated the ion-flow speed  $v_i = \mu E_{dc}$  [Fig. 5(b)] using ion mobility data [36] and assuming room-temperature gas.

The ion-flow speed  $v_i$  was found to be of the order of  $10^2$  m/s in the region of interest, where we observe chains in the experiment in Sec. IV. This region is centered on the midplane at about  $1.5 < r < 3.5$  cm and  $|z| < 0.4$  cm.

For the purpose of interpreting the chain formation observed in this paper, it is significant that the ion-flow speed is very slow. It is comparable to the ion thermal speed  $v_{T,i} \approx 250$  m/s and much slower than the ion acoustic speed  $c_s$ . The Mach number  $M = v_i/c_s$  [Fig. 5(d)] is in the range  $0.02 < M < 0.1$ , in the region of interest.

These calculations assume an argon ion temperature  $T_i \approx 300$  K and the values of the electron temperature  $T_e$  [Fig. 5(c)] computed at each grid point in the simulation. The electron and ion densities, not shown in Fig. 5, were in the range  $n_{e,i} = (1-2) \times 10^{14} \text{ m}^{-3}$  in the region of interest.

From these values we calculated the Debye shielding length  $\lambda_{De,i} = [\epsilon_0 k_B T_{e,i} / (n_{e,i} e^2)]^{1/2}$  yielding  $\lambda_{De} = 1.2 \times 10^{-3}$  m and  $\lambda_{Di} = 9.8 \times 10^{-5}$  m for the electrons and ions, respectively. In the presence of streaming ions the effective shielding is described by a modified Debye shielding length [3,4]  $\lambda_S^2 = \lambda_{De}^2 / [1 + k_B T_e / (k_B T_i + m_i v_i^2)]$ , where  $m_i = 40$  amu is the mass of the argon ions. In the region of interest we obtain  $\lambda_S = 1.0 \times 10^{-4}$  m, which is in good agreement with the linearized Debye length  $\lambda_D = (\lambda_{De}^{-2} + \lambda_{Di}^{-2})^{-1/2} = 9.7 \times 10^{-5}$  m due to the slow ion velocities.

The simulation neglects the influence of dust particles, so that it does not provide exact values for the experiment. Since we rely on the simulation mainly to estimate the Mach number, which varies as the first power of the mobility-limited ion velocity and inversely as the square root of the electron temperature, we should discuss the accuracy of these two quantities. The ion velocity is determined mainly by the gradient of the dc electric potential. We note that the simulation results of Akdim and Goedheer [37], as seen in their Figs. 4 and 5, indicate that the presence of dust alters the gradient of the dc electric potential by a factor of about 2. Thus, neglecting dust in our simulation might contribute an error of a factor

of 2, in the calculation of the Mach number. The electron temperature might also be in error by a factor of 2, since the SIGLO simulation does not include kinetic effects. Thus, our result for the Mach number might have another error of a factor

of  $\sqrt{2}$  due to  $T_e$ . Even with these limitations in mind, we can still be confident that in the presence of dust, the ions in the region of interest flow at a speed  $v_i$  that is much closer to  $v_{T,i}$  than  $c_s$ .

- 
- [1] P. K. Shukla and M. M. Mamun, *Introduction to Dusty Plasma Physics* (IOP, 2002).
- [2] M. Klindworth, O. Arp, and A. Piel, *J. Phys. D: Appl. Phys.* **39**, 1095 (2006).
- [3] I. H. Hutchinson, *Plasma Phys. Controlled Fusion* **47**, 71 (2005).
- [4] I. H. Hutchinson, *Plasma Phys. Controlled Fusion* **48**, 185 (2006).
- [5] M. Lampe, G. Joyce, and G. Ganguli, *IEEE Trans. Plasma Sci.* **33**, 57 (2005).
- [6] V. A. Schweigert, I. V. Schweigert, A. Melzer, A. Homann, and A. Piel, *Phys. Rev. E* **54**, 4155 (1996).
- [7] K. Takahashi, T. Oishi, K. I. Shimomai, Y. Hayashi, and S. Nishino, *Phys. Rev. E* **58**, 7805 (1998).
- [8] A. Melzer, V. A. Schweigert, and A. Piel, *Phys. Rev. Lett.* **83**, 3194 (1999).
- [9] M. Kroll, J. Schablinski, D. Block, and A. Piel, *Phys. Plasmas* **17**, 013702 (2010).
- [10] A. V. Zobnin, A. P. Nefedov, V. A. Sinel'shchikov, O. A. Sinkevich, A. D. Usachev, V. S. Filippov, and V. E. Fortov, *Plasma Phys. Rep.* **26**, 415 (2000).
- [11] G. E. Morfill, H. M. Thomas, U. Konopka, H. Rothermel, M. Zuzic, A. Ivlev, and J. Goree, *Phys. Rev. Lett.* **83**, 1598 (1999).
- [12] A. P. Nefedov *et al.*, *New J. Phys.* **5**, 33.1 (2003).
- [13] H. M. Thomas *et al.*, *New J. Phys.* **10**, 033036 (2008).
- [14] A. Piel, M. Klindworth, O. Arp, A. Melzer, and M. Wolter, *Phys. Rev. Lett.* **97**, 205009 (2006).
- [15] M. H. Thoma, H. Hoefner, M. Kretschmer, S. Ratynskaia, G. E. Morfill, A. Usachev, A. Zobnin, O. Petrov, and V. Fortov, *Microgravity Sci. Technol.* **18**, 47 (2006).
- [16] A. V. Ivlev *et al.*, *Phys. Rev. Lett.* **100**, 095003 (2008).
- [17] K. R. Sütterlin *et al.*, *Phys. Rev. Lett.* **102**, 085003 (2009).
- [18] K. R. Sütterlin, H. M. Thomas, A. V. Ivlev, G. E. Morfill, V. E. Fortov, A. M. Lipaev, V. I. Molotkov, O. F. Petrov, A. Wysocki, and H. Löwen, *IEEE Trans. Plasma Sci.* **38**, 861 (2010).
- [19] K. O. Menzel, O. Arp, and A. Piel, *Phys. Rev. Lett.* **104**, 235002 (2010).
- [20] A. Piel, O. Arp, M. Klindworth, and A. Melzer, *Phys. Rev. E* **77**, 026407 (2008).
- [21] G. Praburam and J. Goree, *Phys. Plasmas* **3**, 1212 (1996).
- [22] D. Samsonov and J. Goree, *Phys. Rev. E* **59**, 1047 (1999).
- [23] M. Kretschmer, S. A. Khrapak, S. K. Zhdanov, H. M. Thomas, G. E. Morfill, V. E. Fortov, A. M. Lipaev, V. I. Molotkov, A. I. Ivanov, and M. V. Turin, *Phys. Rev. E* **71**, 056401 (2005).
- [24] A. M. Lipaev *et al.*, *Phys. Rev. Lett.* **98**, 265006 (2007).
- [25] V. Land and W. J. Goedheer, *New J. Phys.* **9**, 246 (2007).
- [26] V. Land and W. J. Goedheer, *New J. Phys.* **10**, 123028 (2008).
- [27] J. Goree, G. E. Morfill, V. N. Tsytovich, and S. V. Vladimirov, *Phys. Rev. E* **59**, 7055 (1999).
- [28] G. Lapenta, *Phys. Rev. E* **66**, 026409 (2002).
- [29] A. Piel, *Phys. Plasmas* **18**, 073704 (2011).
- [30] I. H. Hutchinson, *Phys. Rev. Lett.* **107**, 095001 (2011).
- [31] M. Lampe, G. Joyce, G. Ganguli, and V. Gavrishchaka, *Phys. Plasmas* **7**, 3851 (2000).
- [32] P. Guio, W. J. Miloch, H. L. Pécseli, and J. Trulsen, *Phys. Rev. E* **78**, 016401 (2008).
- [33] I. H. Hutchinson, *Phys. Plasmas* **18**, 032111 (2011).
- [34] SIGLO-2D, Version 1.1, Kinema Software.
- [35] J. P. Boeuf and L. C. Pitchford, *Phys. Rev. E* **51**, 1376 (1995).
- [36] L. S. Frost, *Phys. Rev.* **105**, 354 (1957).
- [37] M. R. Akdim and W. J. Goedheer, *Phys. Rev. E* **67**, 056405 (2003).